IEEE Access
Multidisciplinary | Rapid Review | Open Access Journal

Received June 24, 2019, accepted August 4, 2019, date of publication August 15, 2019, date of current version August 31, 2019.

Digital Object Identifier 10.1109/ACCESS.2019.2935692

The Joint Impact of Fading Severity, Irregular Constellation, and Non-Gaussian Noise on Signal Space Diversity-Based Relaying Networks

MEHMET CAGRI ILTER[1], HAMZA UMIT SOKUN[2], HALIM YANIKOMEROGLU[2], (Fellow, IEEE), RISTO WICHMAN[1], AND JYRI HÄMÄLÄINEN[3]

[1]Department of Signal Processing and Acoustics, Aalto University, 02150 Espoo, Finland
[2]Department of Systems and Computer Engineering, Carleton University, Ottawa, ON K1S 5B6, Canada
[3]Department of Communications and Networking, Aalto University, 02150 Espoo, Finland

Corresponding author: Mehmet Cagri Ilter (mehmet.ilter@aalto.fi)

This work was supported by the Academy of Finland under Grant 311752 and Grant 287249.

ABSTRACT This work focuses on the interplay between rotation angle, transmit power, fading severity, and noise impairment severity in signal space diversity-based three time-slot decode-and-forward two-way relaying networks. Specifically, we develop a joint design for rotation angle selection and transmit power allocation, while taking into account the performance impact of fading severities on the channels and noise impairment severities on the receivers. To model different severities of fading and noise impairment, Nakagami distribution and additive non-Gaussian noise are used respectively. The objective in doing so is to promote the reliable reception of end-sources, while satisfying individual and total power budgets as well as average error probability. To this end, we start by deriving average error probabilities of end-sources for non-uniform constellations, which capture all possible signal constellations produced by using various rotation angles. Next, we formulate the joint design problem in an optimization form. Unfortunately, the resulting formulation is a non-convex optimization. To find the solution, we resort to numerical optimization. The numerical results not only validate the derived error probability expressions, but also demonstrate the efficacy of the proposed framework and provide useful insights on the interaction between rotation angle, transmit power, fading severities of the channels, and noise impairment severities at the end-sources.

INDEX TERMS Cooperative communication, non-uniform constellation, relaying networks, signal space diversity, decode-and-forward, additive non-Gaussian noise, Nakagami distribution.

I. INTRODUCTION

5G networks are expected to support various services, such as industrial automation and vehicular interconnectivity, which are critically dependent on the availability of wireless links with high reliability [1]. Cooperative communication and signal space diversity (SSD) have been recognized as two effective techniques to enhance transmission reliability at link level in wireless networks. The first achieves spatial diversity by creating a virtual antenna array [2], and the second achieves modulation diversity by applying a certain rotation to a classical signal constellation [3].

In addition to improve the transmission reliability, channel-adaptive transmission schemes were widely used for increasing transmission efficiency at the same time. Design rules for determining modulation order and coding rates based on different channel conditions can be found in [4] and [5]. The examples proposed for fiber optical channels where constellations vary with different channel features were given in [8]. The advantages of signal-to-noise ratio (SNR)-adaptive constellation design over bit-interleaved coded modulation (BICM) coded systems are presented in [9] and the concept of SNR-adaptive transmission with a set of irregular constellations were represented for coded scenarios [10] and for cognitive radio networks in [11].

In the above mentioned constellation design studies, Gaussian noise models were commonly used although various noise models have been proposed for lighting discharge [12], electromagnetic interference and impairment in powerline

The associate editor coordinating the review of this article and approving it for publication was Lei Guo.

communication (PLC) systems [13]. The optimal precoding strategy for MIMO-PLC was investigated in [14] in the context of impulsive noise models. Another impulsive noise model was discussed in direct-sequence spread-spectrum access along with α-stable noise in [12]. Also, Middleton's class-A noise model was discussed for diversity combining schemes in [15]. The new detection method in non-Gaussian noise cases along with Nakagami fading scenarios was investigated in [16]. Within those models, it was very difficult to define model parameters, and the change in noise model may lead to a rethinking of actual signal detection systems. Along these lines, [17] proposed an additive non-Gaussian noise (ANGN) model, which focused on simplicity, robustness, and analytical tractability; the aforementioned noise models can be understood as special cases of this proposed ANGN model.

A. MOTIVATION AND CONTRIBUTION

To leverage spatial and modulation diversities jointly, SSD-based cooperative schemes were discussed in [18]–[22]. They considered various cooperative transmission protocols in one-way and two-way relaying networks with and without relay selection. More specifically, in these schemes, original data symbols were first rotated by a certain angle prior to transmission. This resulted in the information of the original data symbols being distributed over the in-phase and quadrature components of the respective rotated symbols. Then, the components of the rotated symbols were transmitted via the cooperation of the end-sources and the relay(s) so as to ensure that the components experienced different fades. Reference [18]–[21] mostly focused on providing closed-form expressions for error probabilities, assuming that an optimal rotation angle was available. Since this assumption lead to uniformly distributed constellations (after the operations of rotation and interleaving in SSD), it overly simplified the calculation of the closed-form expressions. However, none of these closed-form expressions provide any additional insights on the performance impact of rotation angle selection in the systems. This issue has been addressed by [22]. This paper first generalizes closed-form expressions for error probabilities for the case of arbitrary rotation angle selection. Then, it investigates the joint and individual impacts of rotation angle selection and transmit power allocation on the system performance. Further, it proposes a SNR adaptive SSD-based cooperative transmission scheme for two-way relaying networks.

In the aforementioned works, there are two common assumptions that limit the scope of the validity of the given closed-form expressions for error probabilities:

- All channels are modeled using Rayleigh distribution, viz., considering same level of severity for fading channels.
- There is a basic (impractical) noise model, additive white Gaussian noise (AWGN). However, in practice, wireless systems are often impaired by non-Gaussian noise resulting from factors such as electromagnetic interference, and human-made impulsive noise [12], [15].

In this work, we investigate the joint optimization of rotation angle and power allocation, while taking into account the influence of both the fading severity of the channels and the noise impairment severity at the receivers. To account for the fading severity of the channels in the joint design problem, we utilize a general distribution, viz., Nakagami distribution, to model the fading channel characteristics of links. The Nakagami distribution is parameterized by $m \in [0.5, \infty]$, which measures the ratio of line-of-sight signal power to multi-path power. For instance, when the value of m is set to one, the distribution corresponds to Rayleigh fading (severe fading condition). The severity of fading reduces as the value of m approaches infinity, and lastly, when $m = \infty$, it corresponds to an AWGN channel with no fading [23]. Furthermore, to account for noise impairment severity in the system, we utilized a general noise model proposed in [17], viz., ANGN model, due to simplicity, robustness, and analytical tractability. It is worth mentioning that the AWGN model is a special case of the ANGN model. Broadly speaking, the contributions of the work can be summarized as follows:

- We begin by deriving a closed-form expression for the probability density function (PDF) of the output SNR at the end-sources over the Nakagami fading channels with the existence of ANGN.
- Next, using the derived PDF expressions, a closed-form expression for the average error probabilities of the end-sources for irregular constellations is obtained, which enables us to obtain the optimum rotation angle as a function of SNR.
- Lastly, using the average error probability expressions, we propose an optimization framework that explores the complex interaction among rotation angle selection and transmit power allocation for various SNR values and severity levels of fading and noise impairment. The design objective is to minimize the average error probability of one of the end-sources, while meeting the individual and total power budget constraints and the predefined threshold for the average error probability of the other end-source.

B. PAPER ORGANIZATION

The paper is organized as follows. Section II describes the two-way system model together with the SSD-based cooperative transmission protocol. Section III derives the analytical expressions for the average error probability that provide the basis for the optimization of the rotation angle and transmit power allocation in Section IV. Section IV focuses on the problem of maximizing the transmission reliability. Section V includes numerical analysis and discussions. Lastly, Section VI concludes the work.

II. SYSTEM AND TRANSMISSION MODEL

We consider a system that consists of two end-sources ($\mathcal{A}$ and $\mathcal{B}$) and an intermediate relay ($\mathcal{R}$), see Fig. 1.

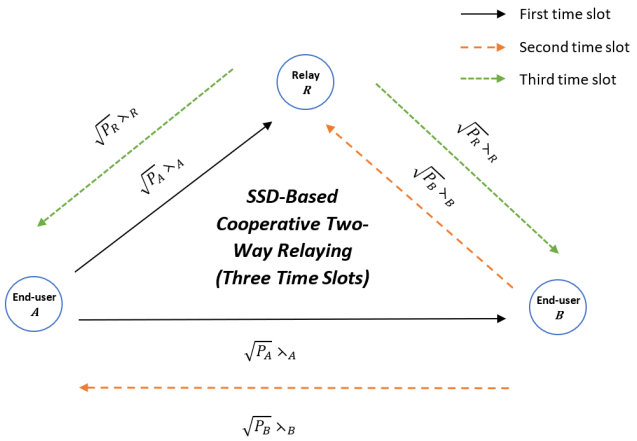

FIGURE 1. An example for the SSD-based cooperative two-way relaying system.

We assume that the channels are reciprocal and modeled by a Nakagami-m random variable with shaping parameters of $\{m_{\mathcal{AB}}, m_{\mathcal{AR}}, m_{\mathcal{BR}}\}$ and average fading powers of $\{\Omega_{\mathcal{AB}}, \Omega_{\mathcal{AR}}, \Omega_{\mathcal{BR}}\}$ for the links of $\mathcal{A} \leftrightarrow \mathcal{R}$, $\mathcal{B} \leftrightarrow \mathcal{R}$, and $\mathcal{A} \leftrightarrow \mathcal{B}$, respectively. It is assumed that the wireless channel coefficients remain constant during one symbol duration.

Similar to [22], in the considered scheme, signal space diversity and a three time-slots cooperative two-way relaying protocol are incorporated to double the number of symbols that are transmitted over three time slots, i.e., four symbols over three time slots. In particular, the original symbols are first rotated by a certain angle before being transmitted from both the end-source $\mathcal{A}$ and the end-source $\mathcal{B}$. Next, the end-source $\mathcal{A}$ and the end-source $\mathcal{B}$ collaborate with the relay $\mathcal{R}$ to transmit the real and imaginary parts of the rotated symbols. A new constellation, χ, is generated by applying a transformation Θ to an ordinary constellation, and the transformation Θ be given as $\Theta = \begin{bmatrix} \cos(\theta) & -\sin(\theta) \\ \sin(\theta) & \cos(\theta) \end{bmatrix}$, where θ is the rotation angle in two-dimensional signal space. A pair of signal points from the rotated constellation, i.e., $s_1^{\mathcal{A}}, s_2^{\mathcal{A}} \in \chi$, which corresponds to the end-source $\mathcal{A}$'s message, is assumed to be transmitted. Note that $s_1^{\mathcal{A}} = \Re\{s_1^{\mathcal{A}}\} + \mathrm{j}\Im\{s_1^{\mathcal{A}}\}$ and $s_2^{\mathcal{A}} = \Re\{s_2^{\mathcal{A}}\} + \mathrm{j}\Im\{s_2^{\mathcal{A}}\}$, where $\Re\{.\}$ and $\Im\{.\}$ represent the in-phase and quadrature components of the corresponding signal points, respectively. After interleaving the components of $s_1^{\mathcal{A}}$ and $s_2^{\mathcal{A}}$, the new constellation point that will be sent from the end-source $\mathcal{A}$ can be written as $\lambda_{\mathcal{A}} = \Re\{s_1^{\mathcal{A}}\} + \mathrm{j}\Im\{s_2^{\mathcal{A}}\}$. Similarly, we assume that $\mathbf{s}^{\mathcal{B}} = (s_1^{\mathcal{B}}; s_2^{\mathcal{B}})$ is a pair of signal points from the rotated constellation, i.e., $s_1^{\mathcal{B}}, s_2^{\mathcal{B}} \in \chi$, which corresponds to end-source $\mathcal{B}$'s message. Again, the constellation point that will be transmitted from the end-source $\mathcal{B}$ is formed by interleaving the components of $s_1^{\mathcal{B}}$ and $s_2^{\mathcal{B}}$ as follows: $\lambda_{\mathcal{B}} = \Re\{s_1^{\mathcal{B}}\} + \mathrm{j}\Im\{s_2^{\mathcal{B}}\}$. We note that $\lambda_{\mathcal{A}}$ and $\lambda_{\mathcal{B}}$ belong to the expanded constellation, Λ, defined as $\Lambda = \Re\{\chi\} \times \Im\{\chi\}$, where $\times$ denotes the Cartesian product of two sets. In this expanded constellation, all members consist of two components, each of which uniquely identifies a particular member of χ. Hence, decoding a member of the expanded constellation results in decoding two different members of the original constellation.

A. COOPERATIVE TRANSMISSION PROTOCOL

In the first time slot, the received signals at end-source $\mathcal{B}$ and relay $\mathcal{R}$ can be written as

$$y^{\mathcal{A}\to\mathcal{B}} = \sqrt{E_{\mathcal{A}}} h_{\mathcal{AB}} \lambda_{\mathcal{A}} + n_{\mathcal{B}}, \quad (1)$$

$$y^{\mathcal{A}\to\mathcal{R}} = \sqrt{E_{\mathcal{A}}} h_{\mathcal{AR}} \lambda_{\mathcal{A}} + n_{\mathcal{R}}, \quad (2)$$

where $E_{\mathcal{A}}$ denotes the transmit power at end-source $\mathcal{A}$. Herein, the probability density functions (PDF) of the noise variables (n_A and n_B) conditioned on g are given as

$$f_{n_i}(n|g) = \frac{e^{-n^H n}}{\pi \sigma_n^2 g}. \quad (3)$$

Herein, g is a non-negative random variable, and σ_n^2 has turned into the variance of pure Gaussian noise for $g = 1$, $i \in \{B, R\}$ [17]. Let suppose that g has Gamma distribution with unit mean and Gamma parameter, k_g, the noise power has become a random variable and its PDF is written as

$$f_g(g) = \frac{k_g^{k_g}}{\Gamma(k_g)} e^{-k_g g} g^{k_g - 1}. \quad (4)$$

In the case of $k_g \to \infty$, (4) leads to a dirac delta function so it yields a Gaussian noise model [17]. This is because some well-known non-Gaussian noise models [17] (i.e. Middleton class-A noise model and Gaussian mixer model) can be included as a special case of (4).

In the second time slot, the received signals at end-source $\mathcal{A}$, $y^{\mathcal{B}\to\mathcal{A}}$, and relay $\mathcal{R}$, $y^{\mathcal{B}\to\mathcal{R}}$, can be written by replacing $\lambda_{\mathcal{B}}$ and $E_{\mathcal{B}}$ which denotes the transmit power at end-source $\mathcal{B}$.

In the third time slot, the new constellation point that will be sent from the relay, $\mathcal{R}$ is formed by interleaving the components of $s_1^{\mathcal{A}}$ and $s_2^{\mathcal{A}}$, and $s_1^{\mathcal{B}}$ and $s_2^{\mathcal{B}}$ as follows:

$$\lambda_{\mathcal{R}} = \frac{1}{\sqrt{2}}\left(\Re\{s_2^{\mathcal{A}}\} + \mathrm{j}\Im\{s_1^{\mathcal{A}}\}\right) + \frac{1}{\sqrt{2}}\left(\Re\{s_2^{\mathcal{B}}\} + \mathrm{j}\Im\{s_1^{\mathcal{B}}\}\right). \quad (5)$$

The received signals at the end-sources can be given as

$$y^{\mathcal{R}\to\mathcal{A}} = \sqrt{E_{\mathcal{R}}} h_{\mathcal{AR}} \lambda_{\mathcal{R}} + \tilde{n}_{\mathcal{A}}, \quad (6)$$

$$y^{\mathcal{R}\to\mathcal{B}} = \sqrt{E_{\mathcal{R}}} h_{\mathcal{BR}} \lambda_{\mathcal{R}} + \tilde{n}_{\mathcal{B}}, \quad (7)$$

where $E_{\mathcal{R}}$ is the transmit power used in the third time slot. Since end-sources $\mathcal{A}$ and $\mathcal{B}$ know their own data, the back-propagating known data can be canceled out, and the modified received signals at the end-sources can be expressed as

$$y^{\mathcal{R}\to\mathcal{A}} = \sqrt{\frac{E_{\mathcal{R}}}{2}} h_{\mathcal{AR}} \left[\Re\{s_2^{\mathcal{B}}\} + \mathrm{j}\Im\{s_1^{\mathcal{B}}\}\right] + \tilde{n}_{\mathcal{A}}, \quad (8)$$

$$y^{\mathcal{R}\to\mathcal{B}} = \sqrt{\frac{E_{\mathcal{R}}}{2}} h_{\mathcal{BR}} \left[\Re\{s_2^{\mathcal{A}}\} + \mathrm{j}\Im\{s_1^{\mathcal{A}}\}\right] + \tilde{n}_{\mathcal{B}}. \quad (9)$$

The received signals at end-source B in the first and third time slots can be given as

$$y^{\mathcal{A}\to\mathcal{B}} = \sqrt{E_{\mathcal{A}}}h_{\mathcal{AB}}\left[\Re\{s_1^{\mathcal{A}}\} + \mathrm{j}\Im\{s_2^{\mathcal{A}}\}\right] + n_{\mathcal{B}}, \quad (10)$$

$$y^{\mathcal{R}\to\mathcal{B}} = \sqrt{\frac{E_{\mathcal{R}}}{2}}h_{\mathcal{BR}}\left[\Re\{s_2^{\mathcal{A}}\} + \mathrm{j}\Im\{s_1^{\mathcal{A}}\}\right] + \tilde{n}_{\mathcal{B}}. \quad (11)$$

By comparing the received signals at user $\mathcal{B}$, it is observed that the received signal from the selected relay contains components of the original signal that are not included in the received signal from user $\mathcal{A}$. Hence, from the point of view of user $\mathcal{B}$, different components of each member of the original signal (i.e., $s_1^{\mathcal{A}}$ and $s_2^{\mathcal{A}}$) are affected by independent channel fading. To detect the original message, end-source $\mathcal{B}$ reorders the received components so that the corresponding components of each signal point in $s^{\mathcal{A}}$ join together.

Considering the existence of the non-Gaussian noise model at the receivers as in (3) and (4), the optimal detection algorithm under this assumption might be questionable. From this perspective, it was already shown that the optimal symbol-wise detection algorithm used in the Gaussian noise model is also optimal for the considered ANGN model [17]. Therefore, end-source $\mathcal{B}$ applies a maximum likelihood (ML) detector on the reordered signal to detect the source message. Hence, end-source $\mathcal{B}$'s ML decision rule can be expressed as follows:

$$\hat{s}_1^{\mathcal{A}} = arg\min_{s_1^{\mathcal{A}}\in\chi}\Big[\Big|\Re\{h_{\mathcal{AB}}^* y^{\mathcal{A}\to\mathcal{B}}\} - |h_{\mathcal{AB}}|^2\sqrt{E_{\mathcal{A}}}\Re\{s_1^{\mathcal{A}}\}\Big|^2 + \Big|\Im\{h_{\mathcal{BR}}^* y^{\mathcal{R}\to\mathcal{B}}\} - |h_{\mathcal{BR}}|^2\frac{E_{\mathcal{R}}}{2}\Im\{s_1^{\mathcal{A}}\}\Big|^2\Big], \quad (12)$$

$$\hat{s}_2^{\mathcal{A}} = arg\min_{s_2^{\mathcal{A}}\in\chi}\Big[\Big|\Im\{h_{\mathcal{AB}}^* y^{\mathcal{A}\to\mathcal{B}}\} - |h_{\mathcal{AB}}|^2\sqrt{E_{\mathcal{A}}}\Im\{s_2^{\mathcal{A}}\}\Big|^2 + \Big|\Re\{h_{\mathcal{BR}}^* y^{\mathcal{R}\to\mathcal{B}}\} - |h_{\mathcal{BR}_b}|^2\frac{E_{\mathcal{R}}}{2}\Re\{s_2^{\mathcal{A}}\}\Big|^2\Big]. \quad (13)$$

Following the same procedure, the detection at end-source $\mathcal{A}$ can be obtained in a similar manner.

III. PERFORMANCE ANALYSIS OVER NAKAGAMI FADING

The end-to-end (E2E) error probability for ith user is expressed as

$$\overline{P}_i(e) = \overline{P}_{off}\overline{P}_{\text{direct}}^{i\to j} + \left(1-\overline{P}_{off}\right)\overline{P}_i(e\,|R), \quad (14)$$

such that $i \neq j,\ j \in \{\mathcal{A},\ \mathcal{B}\}$. Here, $\overline{P}_{off}$ is the probability of the case where the relay remains silent because of erroneous reception of information from a single user or both, $\overline{P}_{\text{direct}}^{i\to j}$ gives the average error probability belonged to the $\mathcal{A}\leftrightarrow\mathcal{B}$ link, and $\overline{P}_i(e\,|\mathcal{R})$ considers the error probability where the relay is actively used at the end user in a cooperative manner.

A. DIRECT LINK CALCULATION

In a direct link scenario, e.g., $\mathcal{A}\to\mathcal{B}$, the received instantaneous SNR at end-source $\mathcal{B}$ can be given by $\gamma_{\mathcal{B}}^{\text{direct}} = E_{\mathcal{A}}|h_{\mathcal{AB}}|^2/g\sigma_n^2$, and the instantaneous error probability expression conditioned on g at end-source $\mathcal{B}$ can be written as,

$$P_{\text{direct}}^{\mathcal{A}\to\mathcal{B}}\left(\gamma_{\mathcal{B}}^{\text{direct}}|g\right) = \sum_{k=0}^{M^2-1}P_k\sum_{\substack{l=0\\l\neq k}}^{M^2-1}\Pr\left[y^{\mathcal{A}\to\mathcal{B}}\in D_{\Lambda(l)}\,|g,\,\Lambda(k)\right], \quad (15)$$

where P_k is the probability of transmitting the k-th symbol, $\Lambda(k)$ is the k-th symbol in the expanded constellation, and $D_{\Lambda(k)}$ is the decision region of the symbol $\Lambda(k)$. Note that $P_{\text{direct}}^{\mathcal{A}\to\mathcal{B}}\left(\gamma_{\mathcal{B}}^{\text{direct}}|g,\,\Lambda(k)\right)$ consists of the sum of all possibilities that a transmitted $\Lambda(l)$ symbol drops into $D_{\Lambda(k)}$. By utilizing the geometric trajectory on 2-D space shown in [24], $\Pr\left[y^{\mathcal{A}\to\mathcal{B}}\in D_{\Lambda(l)}\,|\Lambda(k)\right]$ can be formulated as

$$\Pr\left[y^{\mathcal{A}\to\mathcal{B}}\in D_{\Lambda(l)}\,|g,\,\lambda_{\mathcal{A}}=\Lambda(k)\right] = \sum_{t=1}^{T_l}\pm Q\left(\kappa_1\sqrt{\gamma_{\mathcal{B}}^{\text{direct}}},\kappa_2\sqrt{\gamma_{\mathcal{B}}^{\text{direct}}};\kappa_3\right), \quad (16)$$

where the definition of κ_1, κ_2 and κ_3 are given as[1]

$$\kappa_1 = \pm\sqrt{2}\mathcal{L}_{l,p_t}(\Lambda(k)), \quad (17a)$$

$$\kappa_2 = \pm\sqrt{2}\mathcal{L}_{l,p_{t+1}}(\Lambda(k)), \quad (17b)$$

$$\kappa_3 = \pm\Re\left[c_{l,p_t}, c_{l,p_t}^*\right]. \quad (17c)$$

Herein, T_l denotes the lines bounding the decision region $D_{\Lambda(l)}$, $c_{k,l} = \lambda(l) - \lambda(k)$. In (16), the neighboring decision regions of the symbol $\Lambda(l)$ are expressed by $\Lambda(l)_{\Lambda(p_t)}$ and $\Lambda(l)_{\Lambda(p_{t+1})}$, and $Q(\cdot,\cdot;\cdot)$ denotes the complementary cumulative density function (CCDF) of a bivariate Gaussian variable [25]. The detailed information about the sign $\pm$ and summation terms can be found in [26].

The conditioned average E2E error probability can be obtained by taking the average of instantaneous error probability in (15) with respect to $\gamma_{\mathcal{B}}^{\text{direct}}$, which can be explicitly formulated as

$$P_{\text{direct}}^{\mathcal{A}\to\mathcal{B}}\left(\overline{\gamma}_{\mathcal{B}}^{\text{direct}}|g\right) = \sum_{k=0}^{M^2-1}\sum_{\substack{l=0\\l\neq k}}^{M^2-1}\sum_{t=1}^{T_l}\pm\int_0^{\infty}Q\left(\kappa_1\sqrt{\gamma},\kappa_2\sqrt{\gamma};\kappa_3\right)f_{\text{direct}}^{\mathcal{A}\to\mathcal{B}}(\gamma\,|g)\,d\gamma. \quad (18)$$

Since the fading channels are modeled as Nakagami-m distribution with the Nakagami parameter $m_{\mathcal{AB}}$ and average

[1]Refer to [22] for detailed definitions and intermediate steps for the analysis.

power $\Omega_{\mathcal{AB}}$, the resulting $P_{\text{direct}}^{\mathcal{A}\to\mathcal{B}}\left(\overline{\gamma}_{\mathcal{B}}^{\text{direct}}|g\right)$ can be expressed as

$$P_{\text{direct}}^{\mathcal{A}\to\mathcal{B}}\left(\overline{\gamma}_{\mathcal{B}}^{\text{direct}}|g\right) = \sum_{k=0}^{M^2-1}\sum_{\substack{l=0\\ l\neq k}}^{M^2-1}\sum_{t=1}^{T_l}\sum_{i=1}^{2}\int_0^{\upsilon_i}\frac{d\theta}{2\pi}\left(\frac{\sin^2(\theta)}{\sin^2(\theta)+a_i}\right)^{m_{\mathcal{AB}}}, \quad (19)$$

along with

$$\upsilon_1 = \upsilon(\kappa_1,\kappa_2,\kappa_3), \quad (20a)$$
$$\upsilon_2 = \upsilon(\kappa_2,\kappa_1,\kappa_3), \quad (20b)$$
$$a_1 = \kappa_1\overline{\gamma}_{\mathcal{B}}^{\text{direct}}/(2m_{\mathcal{AB}}), \quad (20c)$$
$$a_2 = \kappa_2\overline{\gamma}_{\mathcal{B}}^{\text{direct}}/(2m_{\mathcal{AB}}) \quad (20d)$$

$$\upsilon(\kappa_1,\kappa_2,\kappa_3) = \begin{cases} \arctan\left(\dfrac{\kappa_1\sqrt{1-\kappa_3^2}}{\kappa_2-\kappa_3\kappa_1}\right), & \kappa_3\kappa_1 \le \kappa_2, \\ \arctan\left(\dfrac{\kappa_1\sqrt{1-\kappa_3^2}}{\alpha_2-\kappa_3\kappa_1}\right)+\pi, & \kappa_2 < \kappa_3\kappa_1, \\ \arctan\left(\dfrac{1+\kappa_3}{1-\kappa_3}\right), & \kappa_1=\alpha_2=0. \end{cases} \quad (20e)$$

Note that the expression of $\overline{\gamma}_{\mathcal{B}}^{\text{direct}}$ is dependent on g since $\overline{\gamma}_{\mathcal{B}}^{\text{direct}} = P_{\mathcal{A}}\Omega_{\mathcal{AB}}/\left(\mathbb{E}\left[g^2\right]\sigma_n^2\right)$ and using [27, Eq.(25)], (19) results in

$$P_{\text{direct}}^{\mathcal{A}\to\mathcal{B}}\left(\overline{\gamma}_{\mathcal{B}}^{\text{direct}}|g\right) = \sum_{k=0}^{M^2-1}\sum_{\substack{l=0\\ l\neq k}}^{M^2-1}\sum_{t=1}^{T_l}\sum_{i=1}^{2}\frac{\mathcal{A}\left(\upsilon\left(\kappa_i,\kappa_{3-i},\kappa_3\right),\xi_i(g)\right)}{2\pi}, \quad (21)$$

where the auxiliary function in (21), $\mathcal{A}(x,y,g)$ is formulated as

$$\mathcal{A}(x,y) = \frac{1}{2\pi}\frac{\sin^2(x)^{(m_{\mathcal{AB}}+1/2)}}{(2m_{\mathcal{AB}}+1)\,y^{m_{\mathcal{AB}}}}F_1\left(m_{\mathcal{AB}}+\frac{1}{2}, m_{\mathcal{AB}}, \frac{1}{2}, m_{\mathcal{AB}}+\frac{3}{2}, -\frac{\sin^2(x)}{y}, \sin^2(x)\right), \quad (22)$$

along with $\xi_1(g) = \frac{\kappa_1\overline{\gamma}_{\mathcal{B}}^{\text{direct}}}{2m_{\mathcal{AB}}}$ and $\xi_2(g) = \frac{\kappa_2\overline{\gamma}_{\mathcal{B}}^{\text{direct}}}{2m_{\mathcal{AB}}}$. Also, $F_1(\cdot,\cdot,\cdot,\cdot,\cdot,\cdot)$ is the Appell hypergeometric function of two variables defined in [28, Eq.(9.180.1)] along with the assumptions of $0 \le \upsilon(\kappa_1,\kappa_2,\kappa_3) < 2\pi$ and $0 \le \upsilon(\kappa_2,\kappa_1,\kappa_3) < 2\pi$. Now, (4) can be used to calculate the unconditioned $\mathcal{A}(x,K)$ such that,

$$\mathcal{A}(x,K) = \int_0^{\infty}\mathcal{A}(x,y)\frac{k_g^{k_g}}{\Gamma(k_g)}e^{-k_g g}g^{k_g-1}dg, \quad (23)$$

and such that $K = \kappa_i^2 P_{\mathcal{A}}\Omega_{\mathcal{AB}}/\left(2\sigma_n^2 m_{\mathcal{AB}}\right)$. Then, $\mathcal{A}(x,K)$ can be calculated as in (24), as shown at the top of the next page, (see Appendix A for details). Note that $\overline{P}_{\text{direct}}^{\mathcal{A}\to\mathcal{B}}$ can be obtained by just replacing $\gamma_{\mathcal{B}}^{\text{direct}}$ with $\gamma_{\mathcal{A}}^{\text{direct}} = P_{\mathcal{B}}\Omega_{\mathcal{AB}}/\left(g^2\sigma_n^2\right)$.

1) GAUSSIAN NOISE ($k_g \to \infty$) WITH INTEGER VALUED m CASES

In the case of the Gaussian noise and integer m values, (24) can be found in a more simplified form, which is [23, Eq.(5A.24)]

$$\begin{aligned}\mathcal{A}(x,y) &= x - \frac{1}{2}\left(\left(1+\text{sign}(x-\pi)\right)\pi + 2\varphi(x,y)\right) \\ &\times\sqrt{\frac{y^2}{2m_{\mathcal{AB}}+y^2}}\sum_{l=1}^{m_{\mathcal{AB}}-1}\binom{2l}{l}\left[4\left(1+\frac{y^2}{2m_{\mathcal{AB}}}\right)\right]^{-l} \\ &-2\sqrt{\frac{y^2}{2m_{\mathcal{AB}}+y^2}}\sum_{l=0}^{m_{\mathcal{AB}}-1}\sum_{p=0}^{l}\binom{2l}{p}\frac{(-1)^{l+p}}{\left[4\left(1+\frac{y^2}{2m_{\mathcal{AB}}}\right)\right]^{l}} \\ &\times\frac{\sin\left(2(l-p)\varphi(x,y)\right)}{2(l-p)}, \end{aligned} \quad (25)$$

where the definition of $\varphi(x,y)$ is given by

$$\begin{aligned}\varphi(x,y) &= \frac{1}{2}\arctan\left(\frac{2\sqrt{\frac{y^2}{2m_{\mathcal{AB}}}\left(1+\frac{y^2}{2m_{\mathcal{AB}}}\right)}\sin(2x)}{\left(1+\frac{y^2}{m_{\mathcal{AB}}}\right)\cos(2x)-1}\right) \\ &+\frac{\pi}{2}\left[1-\frac{1}{2}\left(1+\text{sign}\left(\left(1+\frac{y^2}{m_{\mathcal{AB}}}\right)\cos(2x)-1\right)\right)\right. \\ &\left.\times\,\text{sign}(\sin(2x))\right]. \end{aligned} \quad (26)$$

B. COOPERATIVE LINK CALCULATION

The relay operations depend on a process of decoding the received signals in the first and second time slots from $\mathcal{A} \leftrightarrow \mathcal{R}$ and $\mathcal{B} \leftrightarrow \mathcal{R}$, respectively. The probability of remaining silent in the third time slot for the relay is expressed as $\overline{P}_{off} = 1 - \left(1-\overline{P}_{\text{direct}}^{\mathcal{A}\to R}\right)\left(1-\overline{P}_{\text{direct}}^{\mathcal{B}\to R}\right)$ where $\overline{P}_{\text{direct}}^{\mathcal{A}\to R}$ and $\overline{P}_{\text{direct}}^{\mathcal{B}\to R}$ can be obtained following the same steps already given in (19)-(21) by just replacing $\left(m_{\mathcal{AB}}, \gamma_{\mathcal{B}}^{\text{direct}}\right)$ with $\left(m_{\mathcal{AR}}, \gamma_{\mathcal{AR}}^{\text{direct}} = E_{\mathcal{A}}\Omega_{\mathcal{AR}}/\left(g\sigma_n^2\right)\right)$ for $\mathcal{A} \to \mathcal{R}$ link and $\left(m_{\mathcal{BR}}, \gamma_{\mathcal{BR}}^{\text{direct}} = E_{\mathcal{B}}\Omega_{\mathcal{BR}}/\left(g\sigma_n^2\right)\right)$ for $\mathcal{B} \to \mathcal{R}$ link, respectively.

In a cooperative scenario, the average SER of the cooperative link, e.g., $\mathcal{A} \to \mathcal{R} \to \mathcal{B}$, can be given as

$$\overline{P}_B(e|R) = \sum_{k=0}^{M-1}\sum_{\substack{l=0\\ l\neq k}}^{M-1}\sum_{t=1}^{T_l}\pm\frac{1}{2\pi}\underbrace{\int_0^{\infty}Q\left(\kappa_1\sqrt{\gamma},\kappa_2\sqrt{\gamma};\kappa_3\right)f_{\gamma_{coop}}(\gamma)d\gamma}_{\tau}. \quad (27)$$

Since it is a two-way relaying system that is considered here, the PDF of $\gamma_{\mathcal{RB}}$ is dependent on the average powers used in the first and second time slots. The PDF of the received SNR at the end-source $\mathcal{B}$, $f_{\gamma_{\mathcal{RB}}}(\gamma)$, can be calculated from

$$\mathcal{A}(x,K)=\frac{\sin(x)^{1/2-k_g}K^{-m_{\mathcal{AB}}}\Gamma(k_g+m_{\mathcal{AB}})}{2\pi K^{m_{\mathcal{AB}}}\Gamma\left(k_g\right)\Gamma\left(m_{\mathcal{AB}}+1/2\right)\Gamma\left(k_g\right)}\sum_{s=0}^{\infty}(-1)^{-s}\Gamma\left(1/2+m_{\mathcal{AB}}+s\right)\left(\frac{Kk_g}{\sin^2(x)}\right)^{-k_g-m_{\mathcal{AB}}-s}\times\frac{(m_{\mathcal{AB}})_s\left(m_{\mathcal{AB}}+k_g\right)_s}{s!}\tilde{F}_1\left(\frac{1}{2},m_{\mathcal{AB}}+s+\frac{1}{2};m_{\mathcal{AB}}+s+\frac{3}{2};\sin^2(x)\right). \quad (24)$$

the derivative of the joint CDF of $\mathcal{Z}$ and $\gamma_{\mathcal{RB}}(z,\gamma)$, which are found as follows (See Appendix B for details):

$$f_{\gamma_{\mathcal{RB}}}(\gamma)=\frac{\Gamma(m_{\mathcal{RB}})^{-1}\overline{\gamma}_{\mathcal{AR}}}{\overline{\gamma}_{\mathcal{BR}}+\overline{\gamma}_{\mathcal{AR}}}\left(\frac{m_{\mathcal{RB}}}{\bar{\gamma}_{\mathcal{RB}}^{\text{direct}}}\right)^{m_{\mathcal{RB}}}e^{-\gamma\frac{m_{\mathcal{RB}}}{\bar{\gamma}_{\mathcal{RB}}^{\text{direct}}}}+\frac{\mathcal{K}_{\mathcal{AB}}\overline{\gamma}_{\mathcal{BR}}}{\Gamma(m_{\mathcal{RB}})(\overline{\gamma}_{\mathcal{BR}}+\overline{\gamma}_{\mathcal{AR}})}\left(\frac{m_{\mathcal{RB}}}{\mathcal{K}_{\mathcal{AB}}\bar{\gamma}_{\mathcal{BR}}^{\text{direct}}}\right)^{m_{\mathcal{BR}}}\times e^{-\gamma\frac{m_{\mathcal{RB}}}{\mathcal{K}_{\mathcal{AB}}\bar{\gamma}_{\mathcal{BR}}^{\text{direct}}}}. \quad (28)$$

The PDF of $f_{\gamma_{\mathcal{B}}^{\text{coop}}}^{\mathcal{A}\to\mathcal{R}\to\mathcal{B}}(\gamma)$ is a convolution of $f_{\gamma_{\mathcal{RB}}}(\gamma)$ and $f_{\gamma_{\mathcal{AB}}}(\gamma)$, i.e., $f_{\gamma_{\mathcal{B}}^{\text{coop}}}(\gamma)=f_{\gamma_{\mathcal{R}_i\mathcal{B}}}(\gamma)*f_{\gamma_{\mathcal{AB}}}(\gamma)$ and substituting it into (27), τ in (27) can be formulated as

$$\begin{aligned}&\sum_{i=1}^{2}\int_0^{\upsilon(\kappa_i,\kappa_p,\kappa_3)}\frac{\overline{\gamma}_{\mathcal{AR}}}{\overline{\gamma}_{\mathcal{BR}}+\overline{\gamma}_{\mathcal{AR}}}\left(\frac{\sin^2(\theta)}{\sin^2(\theta)+\kappa_i^2\gamma_{\mathcal{RB}}/2m_{\mathcal{RB}}}\right)^{m_{\mathcal{RB}}}\\&\times\left(\frac{\sin^2(\theta)}{\sin^2(\theta)+\kappa_i^2\gamma_{\mathcal{AB}}/2m_{\mathcal{AB}}}\right)^{m_{\mathcal{AB}}}d\theta\\&+\int_0^{\upsilon(\kappa_i,\kappa_p,\kappa_3)}\frac{\mathcal{K}_{\mathcal{AB}}\overline{\gamma}_{\mathcal{BR}}}{\overline{\gamma}_{\mathcal{BR}}+\overline{\gamma}_{\mathcal{AR}}}\\&\times\left(\frac{\sin^2(\theta)}{\sin^2(\theta)+\kappa_i^2\mathcal{K}_{\mathcal{AB}}\gamma_{\mathcal{BR}}/2m_{\mathcal{RB}}}\right)^{m_{\mathcal{RB}}}\\&\times\left(\frac{\sin^2(\theta)}{\sin^2(\theta)+\kappa_i^2\gamma_{\mathcal{AB}}/2m_{\mathcal{AB}}}\right)^{m_{\mathcal{AB}}}d\theta, \quad (29)\end{aligned}$$

where $p=3-i$.

Considering integer-valued $m_{\mathcal{AB}}$ and $m_{\mathcal{RB}}$, Nakagami fading parameters enable us to utilize from Residue theorem [23, (5.70)], which is given by

$$\prod_{l=1}^{L}\left(\frac{\sin^2(\theta)}{\sin^2(\theta)+c_l}\right)=\sum_{l=1}^{L}\sum_{k=1}^{m_l}A_{k,l}\left(\frac{\sin^2(\theta)}{\sin^2(\theta)+c_l}\right)^{k}, \quad (30)$$

where $A_{k,l}$ is given by [23]

$$A_{k,l}=\frac{\left\{\frac{\mathrm{d}^{m_l-k}}{\mathrm{d}x^{m_l-k}}\prod_{n=1,n\neq l}^{L}\left(\frac{1}{1+c_nx}\right)^{m_n}\right\}\Big|x==c_l^{-1}}{c_l^{m_l-k}(m_l-k)!}. \quad (31)$$

Following this procedure, a closed-form expression for terms seen in (29) can be rewritten in the same form as the ones for $\overline{P}_{\text{direct}}^{\mathcal{A}\to\mathcal{B}}$, which are given (21)-(22), by putting the suitable variables into (30).

IV. MAXIMIZING TRANSMISSION RELIABILITY

Our purpose is to demonstrate that additional performance gains are possible by jointly optimizing the rotation angle and transmit power allocation. To this end, we first introduce the constraints and the design objective.

The growing demand for data traffic increases energy consumption in the system. To limit the total energy consumption over three time slots, we introduce the following constraint: $E_{\mathcal{A}}+E_{\mathcal{B}}+E_{\mathcal{R}}\leq E_T$, where $E_i^{\max}\leq E_T$, $i\in\{\mathcal{A},\mathcal{B},\mathcal{R}\}$, and $E_T\leq E_{\mathcal{A}}^{\max}+E_{\mathcal{B}}^{\max}+E_{\mathcal{R}}^{\max}$. In addition, since each node has a limited battery life in practical systems, the power consumption at the nodes is constrained as $E_i\leq E_i^{\max}$, $i\in\{\mathcal{A},\mathcal{B},\mathcal{R}\}$. Furthermore, the average error probabilities at the end-sources are constrained by a predefined threshold, $\overline{P}_{\text{th}}(e)$, to ensure that transmission reliability for the end-sources is above a certain threshold. The design objective is to minimize the average error probability of one of the end-sources, i.e., to maximize the transmission reliability for this end-source. Then, we formulate the problem for maximizing transmission reliability by jointly optimizing rotation angle and power allocation like this:

$$\begin{aligned}\min_{E_{\mathcal{A}},E_{\mathcal{R}},E_{\mathcal{B}},\,\theta\in(0^\circ,\,45^\circ)}\quad&\overline{P}_{\mathcal{B}}(e) &(32a)\\ \text{subject to}\quad&\overline{P}_{\mathcal{A}}(e)\leq\overline{P}_{\text{th}}(e), &(32b)\\&0<E_i\leq E_i^{\max},\quad i\in\{\mathcal{A},\mathcal{B},\mathcal{R}\}, &(32c)\\&E_{\mathcal{A}}+E_{\mathcal{B}}+E_{\mathcal{R}}\leq E_T. &(32d)\end{aligned}$$

Noting that the constraints (32c) and (32d) are linear, and the objective function and the constraint (32b) are non-convex. Hence, the optimization problem in (32) is non-convex. To obtain the solution for this problem, we resort to numerical optimization using the MATLAB *fmincon* solver which is based on Quasi-Newton updating method.

V. NUMERICAL RESULTS

In this section, we investigate the performance of our proposed joint optimization design and provide numerical results to support its merits. We also consider various fading and noise impairment scenarios. Throughout the numerical analysis, we consider QPSK signalling, and Gray bit-to-symbol mapping in considering scenarios.

Example 1 (Validation of Analytical Error Probability Expression): To validate the analytical expressions proposed for the end-to-end (E2E) average error probabilities in Section III, we consider four different scenarios which include different Nakagami shaping parameter sets,

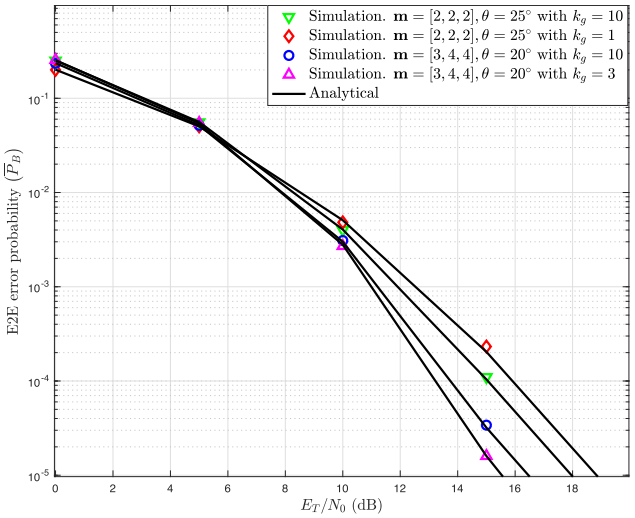

FIGURE 2. Simulation and analytical results comparison for the E2E error probability.

TABLE 1. Optimum rotation angles for different fading severity.

$\mathbf{E_T/N_0}$ (dB)	Scenario-1 θ_{opt} (°)	Scenario-2 θ_{opt} (°)	Scenario-3 θ_{opt} (°)
0	30.42	30.67	30.44
3	29.04	29.01	28.88
6	28.32	28.15	28.05
9	27.94	27.69	27.61
12	27.74	27.45	27.39
15	27.63	27.32	27.28
18	27.57	27.25	27.23
21	27.54	27.21	27.23
24	27.53	27.19	27.23
27	27.52	27.18	27.22
30	27.51	27.18	27.21

$\mathbf{m} = [m_{\mathcal{AB}}, m_{\mathcal{AR}}, m_{\mathcal{BR}}]$, k_g values and given fixed rotation angles, θ. Then, both analytical and simulated results are plotted in Fig. 2. It is worth mentioning that the infinite summation terms in (24) are truncated after the 50th term.

As the figure shows, the analytical results perfectly match the simulation results. Thus, the changes in noise variance (i.e., k_g) and the Nakagami shaping parameter can significantly impact the receiver performance. □

Example 2 (Optimization of Rotation Angle Selection): In this example, we aim to enhance the transmission reliability by solely optimizing rotation angle for the given SNR values. We consider the following scenarios, where $\mathbf{m}$ takes values of [1, 1, 1], [2, 2, 2], and [1, 2, 3] along with $3\Omega_{\mathcal{AB}} = \Omega_{\mathcal{AR}} = 1.5\Omega_{\mathcal{BR}}$ and $k_g \to \infty$. In Fig. 3, the E2E error probability of end-user $\mathcal{B}$ in the considered scheme is plotted. In this figure, the total power budget is assumed to be equally distributed over the end-sources and the relay. We compare two cases: the case when the rotation angle, θ, is fixed for all SNRs, and the case when θ selection is adaptive depending on the SNRs of the channels. For the simulation of the latter case, the optimum values of the rotation angle, θ_{opt}, are used. Noting that the values of θ_{opt} in degree for different E_T/N_0 values are presented in Table 1.

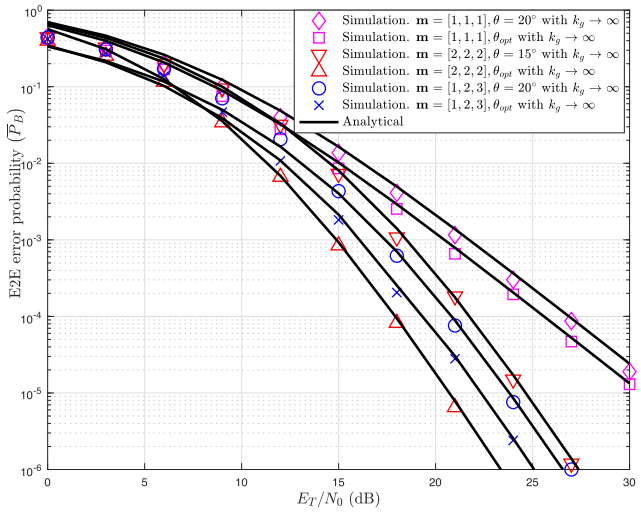

FIGURE 3. Simulation and analytical results comparison with optimal rotation angle values.

TABLE 2. Optimum values from joint optimization.

$E_T/N_0(dB)$	Scenario-1 $\{\theta_{opt}(^\circ), E_{\mathcal{A}}, E_{\mathcal{B}}, E_{\mathcal{R}}\}$	Scenario-3 $\{\theta_{opt}(^\circ), E_{\mathcal{A}}, E_{\mathcal{B}}, E_{\mathcal{R}}\}$
15	{27.58, 0.2671, 0.6419, 0.0900}	{27.12, 0.5545, 0.2992, 0.2274}
18	{27.55, 0.2684, 0.6406, 0.0900}	{26.81, 0.5025, 0.2431, 0.2246}
21	{27.53, 0.4415, 0.3767, 0.1808}	{26.77, 0.3932, 0.2445, 0.2164}
24	{27.52, 0.5538, 0.3144, 0.1308}	{26.73, 0.3485, 0.2402, 0.2304}
27	{27.52, 0.5808, 0.3139, 0.1042}	{26.59, 0.3384, 0.2204, 0.2639}
30	{27.51, 0.5753, 0.3146, 0.1048}	{26.52, 0.3259, 0.2202, 0.3572}

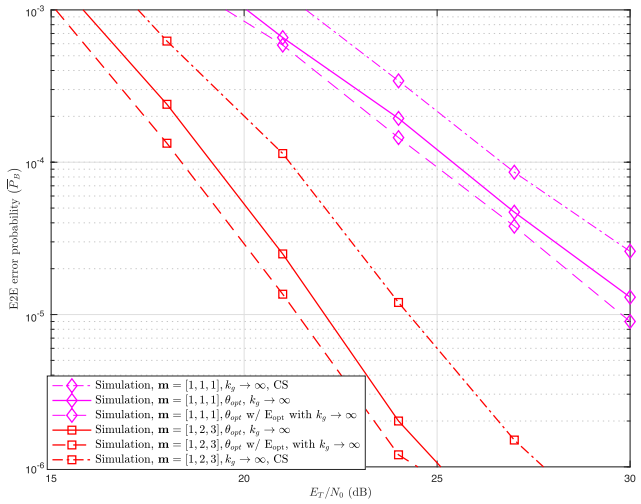

FIGURE 4. Performance comparison of conventional scheme, optimized rotation angle along with equal transmit power allocation, and joint optimized rotation angle and transmit power allocation.

As it can be seen from Fig. 3, the transmission reliability of the system heavily depends on the chosen value of the rotation angle. In addition, the simulation results demonstrate that the considered fading scenario affects the selection of values of the rotation angle for the given SNR. □

Example 3 (Joint Optimization of Rotation Angle Selection and Transmit Power Allocation): Here we investigate the problems associated with angle rotation and power allocation. The improvement achieved by the joint optimization in the

transmission reliability is illustrated in Fig. 4. The optimal values of θ_{opt} and $E_{opt} = \{E_{\mathcal{A}}, E_{\mathcal{B}}, E_{\mathcal{R}}\}$ for various values of E_T/N_0 are shown in Table 2.

As a benchmark model, the E2E error probability of the conventional scheme (CS) is also included to Fig. 4. For a fair comparison, 16-QAM modulation is considered for this CS, which achieves the same spectral efficiency over three time slots. The figure shows that the scheme with optimal rotation angles outperforms the conventional one over the entire range of SNR values. □

VI. CONCLUDING REMARKS

This work builds on the work published in [22], and extends the analysis to include the performance impact of fading severity and noise impairment severity on the SSD-based two-way relaying scheme. We have derived closed-form error probability expressions in presence of Nakagami fading and non-Gaussian noise when two-dimensional non-uniform constellations are adopted for the end-sources. Based on the derived expressions, we develop a framework that jointly optimizes rotation angle selection and transmit power allocation so as to enhance transmission reliability, subject to power budget and average error probability constraints. Subsequently, using this optimization framework, we have provided useful insights on the intricate interplay between rotation angle, transmit power, fading severity, and noise impairment severity. Numerical results confirm our theoretical analysis and show the possible gains that can be obtained by the joint optimization in various scenarios.

APPENDIX A
CALCULATION OF (24)

In this appendix, the derivation of (24) can be represented in a more detailed way. Considering the integral definition of Appell hypergeometric function, $F_1(\cdot,\cdot,\cdot,\cdot,\cdot)$ [29, Eq. (3.1)], (22) can be rewritten as

$$\mathcal{A}(x, y|g) = \frac{1}{2\pi}\frac{\sin^2(x)^{(m_{\mathcal{AB}}+1/2)}}{(2m+1)\,y^{m_{\mathcal{AB}}}}\frac{\Gamma(m_{\mathcal{AB}}+3/2)}{\Gamma(m_{\mathcal{AB}}+1/2)\,\Gamma(1)} \times \int_0^1 \tau^{m_{\mathcal{AB}}-1/2}\left(1+\frac{\sin^2(x)}{y}\tau\right)^{-m_{\mathcal{AB}}} \times \left(1-\sin^2(x)\,\tau\right)^{-1/2} d\tau, \quad (33)$$

such that $y = f(g) = K/g$, $K = \frac{\kappa_I^2 P_{\mathcal{A}} \Omega_{\mathcal{AB}}}{2\sigma_n^2 m_{\mathcal{AB}}}$. Then, unconditioned $\mathcal{A}(x, K)$ can be expressed as

$$\mathcal{A}(x,K) = \frac{1}{2\pi}\frac{\sin^2(x)^{(m_{\mathcal{AB}}+1/2)}}{(2m_{\mathcal{AB}}+1)}\frac{\Gamma(m_{\mathcal{AB}}+3/2)}{\Gamma(m_{\mathcal{AB}}+1/2)\,\Gamma(1)} \times \frac{1}{K^{m_{\mathcal{AB}}}}\int_0^1 \tau^{m_{\mathcal{AB}}-1/2}\left(1-\sin^2(x)\,\tau\right)^{-m_{\mathcal{AB}}} d\tau \times \int_0^\infty \frac{k_g^{k_g}}{\Gamma(k_g)} e^{-k_g g} g^{k_g+m_{\mathcal{AB}}-1}\left(1+\frac{\sin^2(x)}{K}\tau g\right)^{-m_{\mathcal{AB}}} dg. \quad (34)$$

After changing the variable $\sin^2(x)\,\tau g/K$ with t in the second integral above and using the definition of the Tricomi confluent hypergeometric function [30], which is

$$U(z_1, z_2; z_3) = \frac{1}{\Gamma(z_1)}\int_0^\infty e^{-z_3 t} t^{z_1-1}(1+t)^{z_2-z_1-1}\,dt, \quad (35)$$

the closed-form solution of the second integral expression in (34) can be found as

$$\frac{k_g^{k_g} K^{k_g+m_{\mathcal{AB}}}\Gamma(k_g+m_{\mathcal{AB}})}{\Gamma(k_g)\sin^{2k_g+2m_{\mathcal{AB}}}(x)\,\tau^{k_g+m_{\mathcal{AB}}}} \times U\left(k_g+m_{\mathcal{AB}}; k_g+1; \frac{Kk_g}{\sin^2(x)\,\tau}\right). \quad (36)$$

Substituting (36) into (34) yields

$$\mathcal{A}(x,K) = C\int_0^1 \tau^{-k_g-1/2}\left(1-\sin^2(x)\right)^{-1/2} \times U\left(k_g+m_{\mathcal{AB}}; k_g+1; \frac{Kk_g}{\sin^2(x)\,\tau}\right) d\tau, \quad (37)$$

where

$$C = \frac{\sin^2(x)^{(-k_g+1/2)}}{2\pi\,(2m_{\mathcal{AB}}+1)}\frac{k_g^{k_g}}{\Gamma(k_g)}\frac{\Gamma(m_{\mathcal{AB}}+3/2)\,\Gamma(k_g+m_{\mathcal{AB}})}{\Gamma(m_{\mathcal{AB}}+1/2)}. \quad (38)$$

After utilizing Kummer transformation of the Tricomi confluent hypergeometric function [31], $U(z_1, z_2; z_3) = z_3^{1-z_2}U(z_1-z_2+1, 2-z_2; z_3)$, and implementing the Poincare-Type series expansion over the same function, $U(z_1, z_2; z_3) = z_3^{-z_1}\sum_{n=0}^\infty (z_1)_n (z_1-z_2)_n (-z_3)^{-n}/n!$ [32], (34) can be found as

$$\mathcal{A}(x,K) = \frac{\sin(x)^{1/2-k_g} K^{-m_{\mathcal{AB}}}\Gamma(k_g+m_{\mathcal{AB}})}{2\pi K^{m_{\mathcal{AB}}}\Gamma(k_g)\,\Gamma(m_{\mathcal{AB}}+1/2)\,\Gamma(k_g)} \times \sum_{s=0}^\infty (-1)^{-s}\frac{(m_{\mathcal{AB}})_s\,(m_{\mathcal{AB}}+k_g)_s}{s!}\Gamma(1/2+m_{\mathcal{AB}}+s) \times \left(\frac{Kk_g}{\sin^2(x)}\right)^\beta \tilde{F}_1\left(\frac{1}{2}, m_{\mathcal{AB}}+s+\frac{1}{2}; m_{\mathcal{AB}}+s+\frac{3}{2}; \sin^2(x)\right), \quad (39)$$

where $\beta = -k_g - m_{\mathcal{AB}} - s$, $(\cdot)_s$ is the Pochhammer operation and $\tilde{F}_1(\cdot,\cdot;\cdot;\cdot)$ is the regularized hypergeometric function [28].

APPENDIX B
CALCULATION OF (28)

Considering $\mathcal{Z} = \min(\gamma_{\mathcal{A}\to\mathcal{R}}, \gamma_{\mathcal{B}\to\mathcal{R}})$, the joint CDF expression of $\mathcal{Z}$ and $\gamma_{\mathcal{RB}}$ can be formulated as

$$\begin{aligned} &F_{\mathcal{Z},\gamma_{\mathcal{RB}}}(z,\gamma) \\ &= \Pr[\mathcal{Z}\le z, \gamma_{\mathcal{RB}}\le\gamma] \\ &= \Pr[\gamma_{\mathcal{AR}} > \gamma_{\mathcal{BR}}]\Pr[\gamma_{\mathcal{BR}}\le z, \gamma_{\mathcal{RB}}\le\gamma\,|\,\gamma_{\mathcal{AR}} > \gamma_{\mathcal{BR}}] \\ &\quad + \Pr[\gamma_{\mathcal{BR}} > \gamma_{\mathcal{AR}}]\Pr[\gamma_{\mathcal{AR}}\le z, \gamma_{\mathcal{RB}}\le\gamma\,|\,\gamma_{\mathcal{BR}} > \gamma_{\mathcal{AR}}]. \end{aligned} \quad (40)$$

By using the order statistics, $F_{\mathcal{Z},\gamma_{\mathcal{RB}}}(z,\gamma)$ can be rewritten as

$$\begin{aligned} F_{\mathcal{Z},\gamma_{\mathcal{RB}}}(z,\gamma) &= \frac{\overline{\gamma}_{\mathcal{AR}}}{\overline{\gamma}_{\mathcal{BR}}+\overline{\gamma}_{\mathcal{AR}}} F_{\gamma_{\mathcal{AR}}}(z)\, F_{\gamma_{\mathcal{RB}}}(\gamma) \\ &+ \frac{\overline{\gamma}_{\mathcal{BR}}}{\overline{\gamma}_{\mathcal{BR}}+\overline{\gamma}_{\mathcal{AR}}} \big[F_{\gamma_{\mathcal{BR}}}(z)\, u(\gamma/\mathcal{K}_{\mathcal{AB}}-z) \\ &+ F_{\gamma_{\mathcal{BR}}}(\gamma/\mathcal{K}_{\mathcal{AB}})\, u(z-\gamma/\mathcal{K}_{\mathcal{AB}}) - F_{\gamma_{\mathcal{BR}}}(z) \\ &\times \delta(z-\gamma/\mathcal{K}_{\mathcal{AB}})\big], \end{aligned} \tag{41}$$

where $\overline{\gamma}_{\mathcal{RB}} = \mathcal{K}_{\mathcal{AB}}\overline{\gamma}_{\mathcal{BR}}$ and $\mathcal{K}_{\mathcal{AB}} = P_{\mathcal{R}}/P_{\mathcal{B}}$. Herein, $u(\cdot)$ and $\delta(\cdot)$ denote the unit step function and dirac delta function, respectively.

After using the identity $F_{\gamma_{\mathcal{RB}}}(\gamma) = \lim_{z\to\infty} F_{\mathcal{Z},\gamma_{\mathcal{RB}}}(z,\gamma)$ and taking the derivative of $F_{\gamma_{\mathcal{RB}}}(\gamma)$ with respect to γ, the PDF of $\gamma_{\mathcal{RB}}$ can be obtained as (28).

REFERENCES

[1] C.-X. Wang, F. Haider, X. Gao, X.-H. You, Y. Yang, D. Yuan, H. Aggoune, H. Haas, S. Fletcher, and E. Hepsaydir, "Cellular architecture and key technologies for 5G wireless communication networks," *IEEE Commun. Mag.*, vol. 52, no. 2, pp. 122–130, Feb. 2014.

[2] Q. Li, R. Q. Hu, Y. Qian, and G. Wu, "Cooperative communications for wireless networks: Techniques and applications in LTE-Advanced systems," *IEEE Wireless Commun.*, vol. 19, no. 2, pp. 22–29, Apr. 2012.

[3] J. Boutros and E. Viterbo, "Signal space diversity: A power- and bandwidth-efficient diversity technique for the Rayleigh fading channel," *IEEE Trans. Inf. Theory*, vol. 44, no. 4, pp. 1453–1467, Jul. 1998.

[4] M. G. Kim, S. H. Ha, and Y. S. Kim, "A selection method of modulation and coding scheme in cdma2000 1xEV-DV," in *Proc. IEEE Veh. Tech. Conf.*, vol. 2, May 2004, pp. 999–1003.

[5] J. Meng and E. H. Yang, "Constellation and rate selection in adaptive modulation and coding based on finite blocklength analysis and its application to LTE," *IEEE Trans. Wireless Commun.*, vol. 13, no. 10, pp. 5496–5508, Oct. 2014.

[6] A. B. Sediq, P. Djukic, H. Yanikomeroglu, and J. Zhang, "Optimized nonuniform constellation rearrangement for cooperative relaying," *IEEE Trans. Veh. Technol.*, vol. 60, no. 5, pp. 2340–2347, Jun. 2011.

[7] H. Khoshnevis, I. Marsland, and H. Yanikomeroglu, "Design of high-SNR multidimensional constellations for orthogonal transmission in a Nakagami- *m* fading channel," *IEEE Access*, vol. 5, pp. 26623–26638, 2017.

[8] C. Hager, A. Graell i Amat, A. Alvarado, and E. Agrell, "Design of APSK constellations for coherent optical channels with nonlinear phase noise," *IEEE Trans. Commun.*, vol. 61, no. 8, pp. 3362–3373, Aug. 2013.

[9] M. J. Hossain, A. Alvarado, and L. Szczecinski, "Towards fully optimized BICM transceivers," *IEEE Trans. Commun.*, vol. 59, no. 11, pp. 3027–3039, Nov. 2011.

[10] M. C. Ilter and H. Yanikomeroglu, "Convolutionally coded SNR-adaptive transmission for low-latency communications," *IEEE Trans. Veh. Technol.*, vol. 67, no. 9, pp. 8964–8968, Sep. 2018.

[11] T. Aldalgamouni, M. C. Ilter, and H. Yanikomeroglu, "Joint power allocation and constellation design for cognitive radio systems," *IEEE Trans. Veh. Technol.*, vol. 67, no. 5, pp. 4661–4665, May 2018.

[12] A. Rajan and C. Tepedelenlioglu, "Diversity combining over Rayleigh fading channels with symmetric alpha-stable noise," *IEEE Trans. Wireless Commun.*, vol. 9, no. 9, pp. 2968–2976, Sep. 2010.

[13] M. Zimmermann and K. Dostert, "Analysis and modeling of impulsive noise in broad-band powerline communications," *IEEE Trans. Electromagn. Compat.*, vol. 44, no. 1, pp. 249–258, Feb. 2002.

[14] Y. Qian, X. Zhou, J. Li, F. Shu, and D. N. K. Jayakody, "A novel precoding and impulsive noise mitigation scheme for MIMO power line communication systems," *IEEE Syst. J.*, vol. 13, no. 1, pp. 6–17, Mar. 2019.

[15] S. W. Lai and G. G. Messier, "Optimum and suboptimum combining of independent class—A noise channels," in *Proc. IEEE Global Commun. Conf. (GLOBECOM)*, Dec. 2011, pp. 1–5.

[16] X. Zhu, T. Wang, Y. Bao, F. Hu, and S. Li, "Signal detection in generalized Gaussian distribution noise with Nakagami fading channel," *IEEE Access*, vol. 7, pp. 23120–23126, 2019.

[17] R. Annavajjala, C. C. Yu, and J. M. Zagami, "Communication over non-Gaussian channels—Part I: Mutual information and optimum signal detection," in *Proc. IEEE Mil. Commun. Conf. (MILCOM)*, Oct. 2015, pp. 1126–1131.

[18] S. A. Ahmadzadeh, S. A. Motahari, and A. K. Khandani, "Signal space cooperative communication," *IEEE Trans. Wireless Commun.*, vol. 9, no. 4, pp. 1266–1271, Apr. 2010.

[19] T. Lu, J. Ge, Y. Yang, and Y. Gao, "BEP analysis for DF cooperative systems combined with signal space diversity," *IEEE Commun. Lett.*, vol. 16, no. 4, pp. 486–489, Apr. 2012.

[20] O. Amin, R. Mesleh, S. S. Ikki, M. H. Ahmed, and O. A. Dobre, "Performance analysis of multiple-relay cooperative systems with signal space diversity," *IEEE Trans. Veh. Technol.*, vol. 64, no. 8, pp. 3414–3425, Aug. 2015.

[21] E. Erdogan, A. Afana, H. U. Sokun, S. Ikki, L. Durak-Ata, and H. Yanikomeroglu, "Signal space cognitive cooperation," *IEEE Trans. Veh. Technol.*, vol. 68, no. 2, pp. 1953–1957, Feb. 2019.

[22] H. U. Sokun, M. C. Ilter, S. Ikki, and H. Yanikomeroglu, "A spectrally efficient signal space diversity-based two-way relaying system," *IEEE Trans. Veh. Technol.*, vol. 66, no. 7, pp. 6215–6230, Jul. 2017.

[23] M. K. Simon and M.-S. Alouini, *Digital Communication over Fading Channels*, vol. 95. Hoboken, NJ, USA: Wiley, 2005.

[24] L. Szczecinski, S. Aissa, C. Gonzalez, and M. Bacic, "Exact evaluation of bit- and symbol-error rates for arbitrary 2-D modulation and nonuniform signaling in AWGN channel," *IEEE Trans. Commun.*, vol. 54, no. 6, pp. 1049–1056, Jun. 2006.

[25] M. K. Simon, "A simpler form of the Craig representation for the two-dimensional joint Gaussian Q-function," *IEEE Commun. Lett.*, vol. 6, no. 2, pp. 49–51, Feb. 2002.

[26] L. Zhong, F. Alajaji, and G. Takahara, "Error analysis for nonuniform signaling over Rayleigh fading channels," *IEEE Trans. Commun.*, vol. 53, no. 1, pp. 39–43, Jan. 2005.

[27] M. Kang and M.-S. Alouini, "A comparative study on the performance of MIMO MRC systems with and without co-channel interference," in *Proc. IEEE Int. Conf. Commun. (ICC)*, vol. 3, May 2003, pp. 2154–2158.

[28] I. S. Gradshteyn and I. M. Ryzhik, *Table of Integrals, Series, and Products*. New York, NY, USA: Academic, 2014.

[29] Y. A. Brychkov and N. Saad, "Some formulas for the Appell function F1 (a, b, b'; c; w, z)," *Integral Transforms Special Functions*, vol. 23, no. 11, pp. 793–802, Nov. 2012.

[30] F. W. J. Olver, D. W. Lozier, R. F. Boisvert, and C. W. Clark, *NIST Handbook of Mathematical Functions Hardback and CD-ROM*. Cambridge, U.K.: Cambridge Univ. Press, 2010.

[31] N. C. Beaulieu and S. S. Soliman, "Exact analytical solution for end-to-end SNR of multihop AF relaying systems," in *Proc. IEEE Globecom Workshops (GLOBECOM)*, Dec. 2011, pp. 580–585.

[32] M. You, H. Sun, J. Jiang, and J. Zhang, "Effective rate analysis in Weibull fading channels," *IEEE Wireless Commun. Lett.*, vol. 5, no. 4, pp. 340–343, Aug. 2016.

MEHMET CAGRI ILTER received the bachelor's and M.Sc. degrees from Istanbul Technical University, Istanbul, in 2009 and 2012, respectively, and the Ph.D. degree from Carleton University, Ottawa, in 2017. He was a member of Huawei 5G research partnership with Carleton University. He held visiting appointments with the Electrical and Computer Engineering, University of California at Davis, Davis, CA, USA. He is currently a Postdoctoral Fellow with Aalto University, Helsinki, Finland. His research interests include 5G networks, constellation and encoder design, error correcting codes, network coding, network coded cooperation, signal space diversity, applied probability, and the applications of optimization in wireless networks.

HAMZA UMIT SOKUN received the B.Sc. degree (Hons.) in electronics engineering from Kadir Has University, Istanbul, Turkey, in 2010, the M.Sc. degree in electrical engineering from Ozyegin University, Istanbul, Turkey, in 2012, and the Ph.D. degree in electrical engineering from Carleton University, Ottawa, ON, Canada, in 2017. Since 2017, he has been working for Ericsson, Ottawa, ON, Canada. His research interests include wireless communication and networks, signal processing, and machine learning.

HALIM YANIKOMEROGLU (F'17) was born in Giresun, Turkey, in 1968. He received the B.Sc. degree in electrical and electronics engineering from Middle East Technical University, Ankara, Turkey, in 1990, and the M.A.Sc. degree in ECE and the Ph.D. degree in electrical and computer engineering from the University of Toronto, Canada, in 1992 and 1998, respectively. Since 1998, he has been with the Department of Systems and Computer Engineering, Carleton University, Ottawa, Canada, where he is currently a Full Professor. He has supervised 28 M.A.Sc. and 22 Ph.D. students (all completed with theses); several of his Ph.D. students received various medals. He has been one of the most frequent tutorial presenters in the leading international IEEE conferences (31 times). He has had extensive collaboration with the Canadian and international industry. From 2012 to 2016, he led one of the largest academic-industrial collaborative research projects on pre-standards 5G wireless networks. His collaborations with industry have resulted in 31 granted patents. His research interest includes wireless technologies.

Dr. Yanikomeroglu is a Fellow of the Engineering Institute of Canada (EIC) and of the Canadian Academy for Engineering (CAE). He was a recipient of the Carleton University Research Achievement Award, in 2009 and 2018, the Carleton University Graduate Students Association Excellence Award in Graduate Teaching, in 2010, the Carleton University Faculty Graduate Mentoring Award, in 2010, the IEEE Ottawa Section Outstanding Educator Award, in 2014, the IEEE Communications Society Wireless Communications Technical Committee Recognition Award, in 2018, and the IEEE Ottawa Section Outstanding Service Award, in 2018. He served as the General Chair (VTC2017-Fall Toronto and VTC2010-Fall Ottawa) and Technical Program Chair (WCNC 2014 Istanbul, WCNC 2008 Las Vegas, and WCNC 2004 Atlanta) of several major international IEEE conferences. He was the Chair of the IEEE Technical Committee on Personal Communications. He is currently serving as the Steering Committee Chair of IEEE's flagship Wireless Communications and Networking Conference (WCNC). He has served in the editorial boards of the IEEE TRANSACTIONS ON COMMUNICATIONS, the IEEE TRANSACTIONS ON WIRELESS COMMUNICATIONS, and the IEEE COMMUNICATIONS SURVEYS and TUTORIALS. He also served as a Guest Editor in various IEEE journal special issues. He is a Distinguished Speaker of the IEEE Communications Society and the IEEE Vehicular Technology Society. He is a registered Professional Engineer in the Province of Ontario.

RISTO WICHMAN received the M.Sc. and D.Sc. (Tech.) degrees in digital signal processing from the Tampere University of Technology, Finland, in 1990 and 1995, respectively. From 1995 to 2001, he was with the Nokia Research Center as a Senior Research Engineer. In 2002, he joined the Department of Signal Processing and Acoustics, School of Electrical Engineering, Aalto University, Finland, where he has been a Full Professor, since 2008. His research interests include signal processing techniques for wireless communication systems.

JYRI HÄMÄLÄINEN received the M.Sc. and Ph.D. degrees from the University of Oulu, Finland, in 1992 and 1998, respectively. From 1999 to 2007, he was a Senior Specialist and a Program Manager with Nokia, where he worked with various aspects of mobile communication systems and 3GPP standardization. He was a Professor with Aalto University, in 2008, where he was tenured, in 2013. Since 2015, he has been serving as the Dean of the School of Electrical Engineering, Aalto University, that is composed by four departments and the number of staff is currently more than 600 persons including 60 professors. He has authored or coauthored more than 200 scientific publications and 36 U.S. patents or patent applications. His research interests include mobile and wireless systems, with a special focus being in dynamic and heterogeneous networks, including 4-6G, small cells, multi-antenna transmission and reception techniques, scheduling, relays, and many other topics. He is an Expert Member of the Highest Administrative Court of Finland, nominated by the President of Finland.